HHS Public Access

Author manuscript

Adv Biosyst. Author manuscript; available in PMC 2019 May 01.

Published in final edited form as:

Adv Biosyst. 2018 May ; 2(5): . doi:10.1002/adbi.201700259.

Amino Acid Composition Determines Peptide Activity Spectrum and Hot-Spot-Based Design of Merecidin

Xiuqing Wang[1,2], **Biswajit Mishra**[1], **Tamara Lushnikova**[1], **Jayaram Lakshmaiah Narayana**[1], and **Guangshun Wang**[1,*]

[1]Department of Pathology and Microbiology, College of Medicine, University of Nebraska Medical Center, 985900 Nebraska Medical Center, Omaha, NE 68198-5900, USA

[2]Department of Surgery, General Hospital of Ningxia Medical University, Yinchuan 750004, China

Abstract

There is a great interest in developing the only human cathelicidin into therapeutic molecules. The major antimicrobial region of human LL-37 corresponds to residues 17–32. The resultant peptide GF-17 shows a broad spectrum of antimicrobial activity against both Gram-positive and negative bacteria. By reducing the hydrophobic content, we previously succeeded in converting the broad-spectrum GF-17 to two narrow-spectrum peptides (GF-17d3 and KR-12) with activity against Gram-negative bacteria. This study demonstrates that substitution of multiple basic amino acids by hydrophobic alanines makes a broad-spectrum peptide 17BIPHE2 (designed based on GF-17d3) active against Staphylococcal pathogens but not other bacteria tested. Taken together, our results reveal distinct charge and hydrophobic requirements for peptides to kill Gram-positive or Gram-negative bacteria. This finding is in line with the bioinformatics analysis of the peptides in the Antimicrobial Peptide Database (http://aps.unmc.edu/AP). In addition, a hot spot arginine is identified and used to design merecidin with reduced toxicity to human cells. Merecidin protects wax moth larvae (*Galleria mellonella*) from the infection of methicillin-resistant *S. aureus* USA300. These new selective peptides constitute interesting candidates for future development.

Keywords

Antimicrobial peptides; cathelicidin; charge; hydrophobic content; peptide design

1. Introduction

Innate immune peptides (also called antimicrobial peptides), usually cationic and with less than 50 amino acids, are multi-functional peptides discovered in the innate immune systems

*To whom correspondence should be addressed: Department of Pathology and Microbiology, College of Medicine, University of Nebraska Medical Center, 985900 Nebraska Medical Center, Omaha, NE 68198-5900, USA. Phone: (402) 559-4176; gwang@unmc.edu.

Conflict of Interest

The authors declare no competing financial interest. However, 17BIPHE2 and its derivatives such as merecidin reported herein are covered by a US patent 9580472 B2 (issued Feb. 28, 2017).

Supplementary data

Supporting information to this article is provided.

of nearly all life forms, including humans. Their biological activities range from direct antimicrobial effects to immune boosting, making them appealing for developing a new generation of antimicrobials to combat antibiotic-resistant bacteria such as methicillin-resistant *Staphylococcus aureus* (MRSA)[1–6]. Although diverse in terms of source, sequence, activity, and three-dimensional structure, innate immune peptides [3,4] have recently been unified into four classes based on peptide chain connection patterns: linear Class I (UCLL), sidechain-linked class II (UCSS), backbone-sidechain connected Class III (UCSB), and backbone-connected circular peptides (UCBB)[7]. The typical members of UCLL are frog magainins, insect cecropins, human cathelicidin LL-37, and Pro-rich peptides, whereas the members of the UCSS class include both defensin-like peptides and bacterial lantibiotics. Examples of the third peptide class are bacterial daptomycin, colistin, and lasso peptides. Representative members of the fourth class are monkey RTD-1, plant kalata B1, and bacterial enterocin AS-48[5–8]. At present, interest in linear peptides remains high because of their sequence simplicity and ease for chemical synthesis and modification. A variety of methods, including library screening, template-based design, database-aided *ab initio* design, and structure-based design, have been utilized for peptide discovery[9–14].

Human cathelicidin LL-37 is a linear innate immune peptide important for host defense against a variety of invading pathogens, including bacteria, viruses, fungi, and parasites. There are tremendous interests in developing this peptide into antibacterial, antiviral, wound healing, and anticancer therapeutics [10, 13–25]. We have been focusing on this important molecule and achieved the following. First, the major antimicrobial region of human cathelicidin LL-37 was mapped by NMR spectroscopy to residues 17–32 [10]. A synthetic peptide GF-17 based on this region (plus an extra N-terminal glycine) shows a broad-spectrum antimicrobial activity against bacteria, cancer, and viruses, including HIV-1 [10,21]. In the membrane-bound state, GF-17 forms a classic amphipathic helical structure (Figure 1A) [22]. Second, we also designed a selective peptide (GF-17d3) by partially incorporating D-amino acids [10]. GF-17d3 is active against *Escherichia coli* K12 but not *Staphylococcus aureus* USA300 [23]. It has a non-regular amphipathic structure (Figure 1B). Third, library screening revealed stability of GF-17d3 to chymotrypsin, leading to a template for engineering protease-resistant peptides [14]. We also discovered a structure cavity in the 3D structure of GF-17d3, a basis for enhancing the activity of the peptide against methicillin-resistant *Staphylococcus aureus* (MRSA) USA300. Remarkably, the resulting peptide 17BIPHE2 killed all the ESKAPE pathogens, including *Enterococcus faecium*, *Staphylococcus aureus*, *Klebsiella pneumoniae*, *Acinetobacter baumannii*, *Pseudomonas aeruginosa*, and *Enterobacter* species [14]. Moreover, 17BIPHE2 also inhibits biofilm formation both *in vitro* and *in vivo* [14,24]. In addition, this peptide is effective against the 24-h preformed biofilms of *P. aeruginosa*, especially when used in combination with existing antibiotics [25].

This study consists of two parts. The purpose of the first part is to elucidate the effect of basic amino acids on peptide antimicrobial activity and cytotoxicity. For this purpose, alanine scanning was conducted by replacing each of the five basic amino acids with an alanine. Also, double and triple alanine variants were generated by simultaneously changing the two lysines or the three arginines. These studies enabled us to identify a variant that was active only against the two Staphylococcal strains (*Staphylococcus aureus* and

Staphylococcus epidermidis). Because we previously obtained selective peptides against Gram-negative *E. coli* but not *S. aureus* USA300 based on the same peptide template of LL-37, our results underscore the feasibility of converting a broad-spectrum peptide into narrow-spectrum peptides. The second part of this study was built based on the discovery from the first part where we uncovered a hot spot arginine important in determining peptide properties. We then designed a second group of peptides by substituting the hot spot of the sequence with different amino acid analogs. Our study of this group of peptides led to a candidate with similar antimicrobial activity against bacteria, but reduced toxic effects on human cells. Taken together, our results uncover the key elements that determine peptide antibacterial activity spectrum, and indicate a hot spot, identified via alanine scan, is useful for tuning the cell selectivity of a broad-spectrum peptide so that it is less toxic to human cells.

2. Results

2.1. Group I peptides generated via alanine scan

To generate the group I peptides, one to three basic amino acids of 17BIPHE2 were replaced by alanine(s). For convenience, we retained the nomenclature of LL-37 by numbering 17BIPHE2 (sequence GX^{18}K^{19}R$\underline{L}$VQ^{23}R$\underline{L}^{25}$KDX$\underline{L}^{29}$RNLV-NH_2, X = biphenylalanine, D-amino acids for underlined L) from residue 17 to 32 (The N-terminal glycine was appended artificially as it appears at the N-terminus of many natural peptides). There are five basic amino acids in this peptide: K18, R19, R23, K25, and R29, each of which was substituted by an alanine, leading to five different peptide variants. Antimicrobial activity of the five alanine variants of 17BIPHE2 was evaluated using the established microdilution method by using exponential phase bacteria in tryptic soy broth (TSB) [14]. These peptide variants (>95% pure; Genemed Synthesis Inc., TX) displayed minimal inhibitory concentrations (MICs) comparable to the wild type 17BIPHE2 against a panel of pathogens, including *S. aureus* USA300, *S. aureus* UAMS-1, *P. aeruginosa*, *A. baumannii*, *K. pneumoniae*, *E. faecium*, *E. coli,* and *Staphylococcus epidermidis* (Table 1). In addition, pH and salts had little effect on the MIC values of 17BIPHE2 against *S. aureus* USA300 (Figure S1 and Table S2). The robust MICs of 17BIPHE2 in killing various bacteria provide an advantage over its parent peptide LL-37, whose activity is known to be heavily influenced by pH, salts, and media conditions [26,27]. However, pH clearly influenced the MICs of the peptide when the two lysines or three arginines were all replaced with alanines (Figure S1A). Similar trends were observed with GF-17 and its variants. While the single alanine variants were not susceptible, GF-17Q2 (two lysines were changed to glutamines) and GF-17Q3 (three arginines were changed to glutamines) became more sensitive to the effect of pH (Figure S1B). Interestingly, 17BIPHE2 became active only against Gram-positive *S. aureus* USA300 and *S. epidermidis* after the three arginines were substituted by alanines (17BIPHE2-3RA in Table 1). Thus, the three positively charged arginines are significant in inhibiting Gram-negative bacteria *E. coli*, *P. aeruginosa*, *K. pneumoniae*, and *A. baumannii* as well as Gram-positive bacteria *S. aureus* UAMS-1 and *E. faecium*. Our results underscore the feasibility to modulate the activity spectrum of 17BIPHE2. The new peptide 17BIPHE2-3RA can be interesting to selectively eliminate those staphylococcal strains.

Next, we compared the membrane permeation efficiency of 17BIPHE2 and its alanine variants by fluorescence spectroscopy in the presence of a probe molecule. When bacterial membranes are compromised, membrane-impermeable propidium iodide (PI) will enter bacteria and bind to DNA, leading to a rapid increase in fluorescence. While most of the peptide variants of 17BIPHE2 permeated the membranes of *E. coli* ATCC 25922 comparable to the wild type, a change of R23 to alanine (i.e., the R23A variant) caused a more pronounced delay and reduced increase in fluorescence (Figure 2A, red curve). Likewise, the same R23 in the helical peptide GF-17 was previously found to be critical for permeating the *E. coli* membranes [22]. Hence, the cationic R23 residue in both GF-17 and 17BIPHE2 is important in killing Gram-negative *E. coli*, despite different backbone structures: helical for GF-17 and non-helical for 17BIPHE2 (Figure 1, A & B). In contrast, we obtained opposite results for 17BIPHE2 variants when Gram-positive *S. aureus* USA300 was used in the same experiment. The R23 and K25 single alanine variants became more powerful than other Group I single alanine peptide variants in permeating the *S. aureus* membranes (Figure 2B, red and purple curves).

The hemolytic experiments were conducted as described to gauge peptide cytotoxicity [14]. We evaluated hemolysis of 17BIPHE2 and its variants at two concentrations of blood cells: (Fig. 3A) 0.5% (v/v) and (B) 2%. Under both conditions, the single alanine variants generally became more hemolytic than the wild type 17BIPHE2 (Figure 3, black). The order of hemolytic ability is 17BIPHE2-K25A > 17BIPHE2-R23A > 17BIPHE2-K18A > 17BIPHE2-R19A > 17BIPHE2-R29A > 17BIPHE2, indicating that R23 and K25 alanine variants are more hemolytic. As a comparison, we also tested the hemolytic ability of the single alanine variants of GF-17 (Figure S2B). The hemolytic order is GF-17K25A > GF-17R23A > GF-17K18A > GF-17R29A > GF-17R19A > GF-17. Thus, the K25A and R23A variants of GF-17 were also more toxic to human red blood cells. It appears that changes of R23 or K25 to an alanine might have made the peptide more hydrophobic. To provide additional evidence for this, we measured the HPLC retention times of these peptides. Although there is no exact one-to-one correlation between the HPLC retention time and hemolytic concentration of the entire group of peptides, some general trends are evident. For example, double and triple alanine variants are more hydrophobic than the single alanine variants according to HPLC retention times (Table S3). Furthermore, all the alanine variants are more hydrophobic than the wild type peptide. In addition, the higher hydrophobicity of the 17BIPHE2-R23A and 17BIPHE2-K25A variants is also consistent with their HPLC retention times we measured (Table S3). Since a change of R23 of 17BIPHE2 or GF-17 can influence both antimicrobial and hemolytic activities, this arginine is proposed to be a hot spot residue.

2.2. Group II peptides generated by changing the hot spot residue R23 of 17BIPHE2

We reasoned that such a hot-spot arginine of 17BIPHE2 would allow us to modulate the peptide properties. Since a change of R23 to a hydrophobic alanine made 17BIPHE2 rather hemolytic (Figure 3), we attempted other changes. When R23 was substituted by a polar serine S23, the resulting peptide R23S became 2–4 fold less active, and retained the same hemolytic ability as 17BIPHE2 (Table 2). We then replaced R23 of 17BIPHE2 with L-ornithine (O). This R23O peptide retained identical MIC values against *S. aureus*, *E. coli*,

and *P. aeruginosa*, although its MIC against *K. pneumonia* was increased by four-fold (Table 2). Significantly, the hemolysis of R23O (HL_{50} 300 μM) was reduced by nearly 3 fold compared to 17BIPHE2 (HL_{50} 110 μM, Table 2). To substantiate this reduced toxicity, we also used human HaCaT cells. In agreement, R23O was also less toxic to HaCaT cells than 17BIPHE2 (Figure 4). The IC_{50} values (i.e., the peptide concentration that causes 50% cell death) for HaCaT cells were estimated to be 24 μM for 17BIPHE2 and 48 μM for R23O. Because the R23O peptide showed similar MICs against several bacteria, but gained additional cell selectivity, we hereby refer to R23O as merecidin, a 17BIPHE2 analog designed based on the *mere* human catheli*cidin* LL-37. It should be pointed out that an attempt to improve cell selectivity of 17BIPHE2 by changing larger V21 to smaller A21 to reduce the peptide hydrophobicity (a classic approach) did not work (V21A in Table 2).

2.3. Comparison of merecidin with 17BIPHE2

To further compare merecidin with 17BIPHE2, we also conducted additional experiments. The bacterial CFU after 15 min or 60 min killing were quantitated by colony counting. Figure 5 presents the results for the two peptides against *S. aureus* USA 300 (A) or *E. coli* ATCC 25922 (B). At 15 min, 17BIPHE2 at 2 × MIC killed 38% of *S. aureus*, while merecidin killed 31% (Figure 5). Likewise, 17BIPHE2 at 4 × MIC killed 99% of *E. coli*, whereas merecidin killed 87%. At 60 min, 17BIPHE2 was also slightly more efficient than merecidin in killing *S. aureus*. However, no colony was observed on the petri dishes in the case of *E. coli* after treatment with the peptides for 60 min. It appears that 17BIPHE2 is slightly more efficient than merecidin in killing the planktonic bacteria *E. coli* and *S. aureus*.

We also compared the antibiofilm capability of 17BIPHE2 (Figure 6, A–C) and merecidin (Figure 6, D–F). Biofilm formation usually involves the initial bacterial attachment to the surface, growth and maturation stages [28,29]. Similar to 17BIPHE2 (Figure 6A), merecidin showed a clear inhibitory effect (~50%) on the *S. aureus* adhesion even at 3.1 μM (Figure 6D). It seems that 17BIPHE2 is more effective in inhibiting biofilm formation. While 17BIPHE2 worked at 6.25 μM (Figure 6B), merecidin entirely inhibited biofilm growth at 12.5 μM (Figure 6E). Likewise, 17BIPHE2 disrupted the majority of the 24 h established biofilms of *S. aureus* USA300 at 3.1 μM (Figure 6C), whereas merecidin was able to achieve a similar level at 12.5 μM (Figure 6F). These results indicate that merecidin and 17BIPHE2 have comparable ability in inhibiting bacterial adhesion, although 17BIPHE2 is slightly stronger than merecidin in biofilm inhibition and disruption.

It is assumed that cationic antimicrobial peptides kill Gram-negative bacteria by interaction with the outer membrane (OM) layer first and then the inner membrane (IM) layer. To provide insight into the differences in bacterial killing by 17BIPHE2 and merecidin, we also measured the binding ability of these two peptides to LPS (the OM component of Gram-negative bacteria). Using a commercial Kit, we found that 17BIPHE2 appeared to bind to LPS slightly better than merecidin (Figure 7). This experiment would suggest that arginine at position 23 of the peptide is slightly more effective than ornithine in recognizing LPS on the outer membranes of Gram-negative bacteria such as *E. coli*. Note that such a small difference is real, although statistically insignificant.

We also compared membrane permeation of merecidin and 17BIPHE2 using both *E. coli* and *S. aureus*. Two systems were tested in the case of *E. coli*. First, we used the *E. coli* ML-35p strain reported by the lab of Lehrer (see the Method section) [30]. After peptide treatment, 17BIPHE2 was able to permeate the outer membrane (indicated by the fluorescence increase of the nitrocefin probe) slightly more efficiently than merecidin at 6.2 μM (Figure 8A). Likewise, the same difference remained when the two peptides were permeating the inner membrane (Figure 8B). Similar trends were also observed at a peptide concentration of 3.1 μM (not shown). To further validate this observation, we also used the PI probe. In the case of *E. coli* ATCC 25922, there was a clear difference in membrane permeation when the two peptides were administered at 6.2 μM (Figure 9A). At 12.5 μM, 17BIPHE2 was 10 min faster in reaching the maximal membrane permeation than merecidin (not shown). Thus, 17BIPHE2 is slightly more potent than merecidin.

We also compared the membrane permeation using *S. aureus* USA300. 17BIPHE2 (Figure 9B cyan) was slightly better than merecidin (Figure 9 green) in permeating the bacterial membranes when treated at 3.1 μM, indicating that arginine (in 17BIPHE2) is better than ornithine (in merecidin) in membrane permeation as well. To further validate the membrane targeting of the peptides, we also included into the membrane permeation experiment a panel of antibiotics with a defined mechanism of action. Both 17BIPHE2 and merecidin are more potent in permeating the membrane of *S. aureus* USA300 than daptomycin (Figure 9 blue), a membrane active peptide antibiotic in clinical use. In contrast, non-membrane-active antibiotics, such as vancomycin (purple), which inhibits cell wall synthesis, and rifamycin (greenish yellow), which inhibits RNA polymerase, showed no membrane permeation under the same conditions, similar to the untreated *S. aureus* USA300 (red). We conclude that both 17BIPHE2 and merecidin acted on the membranes of bacteria. In the case of *S. aureus* USA300, the membrane permeation ability of these two peptides is superior to daptomycin.

Finally, we demonstrated the *in vivo* efficacy of merecidin using the wax moth *Galleria mellonella* model [31]. As a comparison, 17BIPHE2 was also included. The effects of the compound in protecting the insects from bacterial infection are evident (Figure 10). In the absence of the peptide, an inoculation of *S. aureus* USA300 at 10^6 CFU per insect led to the death of animals with time, whereas no animals died in the untreated group or the PBS treated group, implying bacterial infection was responsible for the death of wax moths. However, the deaths of animals were reduced when they were treated with a single dose of merecidin or 17BIPHE2 2 h ahead of bacterial infection (Figure 10). Notably, peptide treatment alone did not cause animal death, indicating the lack of acute toxicity.

3. Discussion

Human cathelicidin LL-37 is a widely studied peptide owing to its multiple functional roles, such as antimicrobial, antibiofilm, immune modulation, and angiogenesis [13–25]. The structural basis for antimicrobial activity of LL-37 has been elucidated [32]. The long helix covering residues 2–31 is responsible for binding to both the outer and inner membranes of Gram-negative bacteria. Structurally, the two helical domains of LL-37 we found[32] provide structural insight into synergistic binding to LPS previously observed by Lehrer and colleagues [33].

The central helical domain of LL-37 is established as a critical region that determines its antimicrobial, antiviral and antibiofilm potency as well as immune modulation (reviewed in ref. [16]). Our studies also reveal the different requirements of the peptide for killing Gram-negative or Gram-positive bacteira. On one hand, basic charges are critical to kill Gram-negative bacteria. For instance, in the case of Gram-negative *A. baumannii*, MIC doubled for the single alanine variant and further reduced when two basic lysines were replaced with alanines. When the three basic arginines were all changed to alanines, the peptide lost its activity against all the Gram-negative strains investigated here (Table 1 and supporting Table S4 containing the MIC data for additional clinical strains of *A. baumannii*). However, single, double, or triple alanine substitions had little effect on antibacterial activity against Gram-positive *S. aureus* USA300 and *S. epidermidis* (Table 1). Such an activity spectrum for the triple alanine variant is reminiscent of our database designed peptide DFTamP1 that is active only against Gram-positive *S. aureus*, but not Gram-negative bacteria tested[11]. Correspondingly, we found that the physical properties of this triple arginine variant of 17BIPHE2 (net charge +2 and hydrophobic content 64%) are remarkably similar to DFTamP1 (net charge +2 and 61% hydrophobic leucines). This observation is supported by additional activity data for DFTamP1 in Table S5. On the other hand, we previously observed a different effect for changing hydrophobicity. A decrease in peptide hydrophobicity (without touching charged residues) makes two LL-37 peptides active against Gram-negative *E. coli,* but not Gram-positive *S. aureus* [10,32]. In the case of KR-12, the minimal antibacterial peptide of LL-37, the helical backbone structure is maintained and a decrease in peptide hydrophobicity results from hydrophobic amino acid truncation from the peptide termini [32]. In the case of GF-17d3 (previously called dLL-37(17–32)), the reduction in peptide hydrophobicity results from a change in the peptide backbone structure [10]. This change in backbone structure causes an incoherent side chain packing on the hydrophobic surface, leading to a decrease in peptide hydrophobicity and loss of activity against all the Gram-positive bacteria, including *S. aureus*, *S. epidermidis*, and *E. faecium* (new data in Table S5). These results underscore the importance of hydrophobic amino acids for designing peptides to combat *S. aureus*, especially MRSA, whereas positively charged lysines and arginines are significant in killing Gram-negative bacteria.

To further support this notion, we also analyzed the statistical data of naturally occurring antimicrobial peptides registered in the Antimicrobial Peptide Database (APD; http://aps.unmc.edu/AP) [8]. As of November 2017, there are 269 peptides annotated to have activity against mainly Gram-negative bacteria and 485 peptides active against primarily Gram-positive bacteira. On average, peptides active against Gram-positive bacteria have a net charge of +2.4 and a hydrophobic content of 42.6%. Anti-Gram negative bacterial peptides, however, have an averaged net charge of +3.3 and a hydrophobic content of 36.26 (Table 3). Therefore, peptides active against Gram-negative bacteria tend to have a higher net charge than those against Gram-positive bacteria, while an opposite trend is true of hydrophobic content. These results are consistent with our contention that peptides active against Gram-negative or positive bacteria have different requirements for peptide parameters in terms of net charge and hydrophobicity. Such a finding may be useful in guiding the design of peptides with a desired activity spectrum against bacteria.

In addition, certain residue in cationic antimicrobial peptides could play a more important role than others in bacterial killing. Using the major antimicorbial region of LL-37, we showed the significance of R23 of the helical peptide GF-17 for membrane permeation and bacterial killing [22]. Remarkably, R23 also remains critical in a non-helical peptide 17BIPHE2 (Figure 1). Thus, the same amino acid can be important in peptides with different backbone structures. To elucidate the structural basis for this, we studied the space-filling models of GF-17 (Figure 1C) and 17BIPHE2 (Figure 1D). Remarkably, the five cationic amino acids have nearly identical sidechain orientations in these two structures, with R23 and K25 (in the middle) being more adjacent to the hydrophobic surface (green). Thus, a substitution of basic R23 or K25 with an alanine would widen the hydrophobic surface of the peptide. Indeed, both the R23A and K25A variants became more hydrophobic than other variants (Table S3). Such a structural location of the side chains of R23 and K25 in 17BIPHE2 and GF-17 (Figure 1) would also make the alanine variants of these two sites more hemolytic to human red blood cells as we observed in Figure 3. These results validated the interfacial locations of R23 and K25 in the amphipathic structures of both GF-17 and 17BIPHE2 (Figure 1). We propose that the increased hydrophobicity of the peptide is also responsible for increased membrane permeation of *S. aureus* by the R23 or K25 variants (Figure 2B). Such a location of the basic arginine R23 also explains its critical role in permeating the *E. coli* membranes (Figure 2A). In the *E. coli* case, the R23 is so powerful in membrane permeation that it shadowed the outcome of K25A mutation. Since a single alanine substitution or charge swap did not change the peptide helical conformation [34,35], it is the interfacial location of R23[36], rather than the backbone structure, that determines the membrane permeation ability of these two groups of peptides. Indeed, the KR-12R23A and KR-12K25A variants are less helical, indicating their significance in binding to phosphatidylglycerols[34]. It should be pointed out that, however, the backbone structure of the peptide influences peptide stability. In PBS buffer, 17BIPHE2, but not GF-17, is resistant to the action of several proteases, including chymotrypsin, pathogen *S. aureus* V8 protease, and fungal protease K [14].

Interestingly, the properties of 17BIPHE2 can be modulated by changing the hot spot residue, laying the basis for us to improve the cell selectivity index of the peptide (Table 2). When ornithine was utilized to replace arginine, the peptide retained its antimicrobial and antibiofilm activities to a large extent. We validated that R23 in 17BIPHE2 is important for binding to the outer membrane component LPS as well as in permeating the outer and inner membranes of Gram-negative bacteria. The reduced interactions of ornithine than arginine with bacterial outer and inner membranes explain why merecidin showed slightly reduced killing efficiency than 17BIPHE2. Consistent with in vitro data, merecidin and 17BIPHE2 showed a similar protective effect on the moths from *S. aureus* infection, indicating the therapeutic potential of both peptides. These results underscore the interplay between bacterial killing and cytotoxicity. When the peptide is more efficient in killing and membrane permeation (Figures 5, 6, & 8,9), it is also more toxic to human cells (Table 2 and Figure 4). Although bacterial killing and membrane permeation of merecidin are slightly reduced compared to 17BIPHE2, this decrease is affordable because merecidin remains highly potent with membrane-permeation ability better than daptomycin, a peptide antibiotic for treating Gram-positive *S. aureus* infections.

4. Conclusion

This study contributes to the antimicrobial peptide field in three aspects. First, we elucidated the key elements for killing Gram-positive or negative bacteria. Our results underscore the general importance of positively charged residues of the LL-37 derived peptides in killing Gram-negative bacteria and a higher peptide hydrophobicity in killing Gram-positive bacteria. Our observations form the basis for us to tune the activity spectrum of the broad spectrum peptides derived from human cathelicidin LL-37. While KR-12 and GF-17d3) [10,30] are primarily active against mainly Gram-negative bacteria, 17BIPHE2-3RA is mainly active against Staphylococcal pathogens. Thus, amino acid composition is an important determinant of peptide antibacterial activity spectrum. Second, through alanine scan of basic amino acids, our study also uncovers a hot spot arginine in a non-helical peptide 17BIPHE2. Since the same hot spot also exists in a helical template GF-17, it is the interfacial location, rather than the backbone structure, that determines their properties (Figure 1). Third, basic amino acids in antimicrobial peptides are not equally important and the identification of the hot spot lays a basis for our peptide engineering. The resultant peptide merecidin retains the same or similar MICs, slightly reduced killing efficiency, but reduced toxicity. Collectively, our results shed light on the fundamental relationship between peptide composition and activity spectrum. Our findings summarized herein may be utilized to design more selective peptides (narrower activity spectrum to bacteria or reduced toxicity to human cells) as well as predict the antimicrobial activity spectrum of newly identified peptides. The interesting candidates derived from human cathelicidin LL-37 may be further developed for treating infections caused by different types of antibiotic-resistant pathogens.

5. Materials and Methods

5.1. Bacteria strains

The bacterial strains used here included methicillin-resistant *Staphylococcus aureus* USA300, clinical strain *Staphylococcus aureus* UAMS-1, *Staphylococcus epidermidis* 1457, lab strain *Escherichia coli* ATCC 25922, *Pseudomonas aeruginosa* PAO1, *Acinetobacter baumannii* clinical strains, *Klebsiella pneumoniae* ATCC 13883, and *Enterococcus faecium* ATCC 51559. All the bacteria were obtained from the ATCC or the UNMC clinical laboratory. The laboratory, where the work was conducted, has a BSL-2 permission to grow and use these bacteria for antimicrobial assays. All personnel are trained and required to pass the biosafety exam before they can conduct the assays.

5.2. Minimal inhibitory concentration (MIC) assays

The antimicrobial activity of peptides was evaluated using the standard CLSI broth microdilution protocol with minor modifications as described [14, 37]. In brief, exponential phase bacteria at 10^6 CFU were incubated with serially diluted peptides overnight for ~20 h at 37°C. The plates were read on a ChroMate 4300 Microplate Reader at 630 nm (GMI, Ramsey, MN). The MIC was defined as the lowest peptide concentration that fully inhibited bacterial growth. In addition, the effects of pH (6.8, 7.4 and 8.0) and 100 mM sodium chloride (NaCl) on MICs against *S. aureus* USA300 were also evaluated.

5.3. Bacterial killing by colony counting

As the case of antibacterial assays above, bacteria (e.g., *S. aureus* and *E. coli*) were grown to the exponential stage and diluted to 10^6 CFU/mL. Bacterial killing was then initiated by treating the culture with peptides. An aliquot of the culture was taken and spread on LB plates. The plates were incubated at 37°C overnight followed by colony counting.

5.4. Antibiofilm assays

Three types of experiments were conducted to evaluate the antibiofilm activity of these peptides against *S. aureus* USA300, which was grown in TSB in flat bottom, 96 wells, polystyrene microtiter plates (Corning Costar Cat No. 3595) [24–27].

5.4.1. Inhibition of bacterial attachment—The first experiment measures to what extent the peptide can inhibit bacterial attachment, the first step for biofilm formation. In short, overnight cultures of *S. aureus* USA300 were grown in TSB media to an optical density (600 nm) of ~1.0. 180 μL of this culture was added to each well of the microtiter plates containing 20 μL of 10× peptide solution. The plates are then incubated at 37°C for 1 h. Media with bacteria were than pipetted out and chambers were washed with 1× PBS to remove unattached cells. Quantitative evaluation of the inhibition of biofilms was done by XTT [2,3-bis(2-methyloxy-4-nitro-5-sulfophenyl)-2H-tertazolium-5-carboxanilide] assay following manufacture instructions with modifications. 180 μL of fresh TSB and 20 μL of XTT solution were added to each well and the plates were again incubated for 2 h at 37°C. Absorbance at 450 nm (only media with XTT containing wells served as the blank) was obtained using a ChromateTM microtiter plate reader. Percentage biofilm growth for the peptide was plotted assuming 100% biofilm growth is achieved on the bacterial wells without peptide treatment.

5.4.2. Inhibition of biofilm growth—In brief, *S. aureus* USA300 (10^5 CFU/mL) was made form exponentially growing bacteria in fresh TSB media. 180 μL of this bacterial culture was added to each well of the microtiter plates containing 20 μL of 10× peptide solution. The plates were then incubated at 37°C for 24 h. Subsequently, inhibition of the biofilm formation by the peptides was quantitated using XTT as detailed above.

5.4.3. Preformed biofilm disruption—To evaluate the biofilm-disrupting property, *S. aureus* USA300 (10^5 CFU/mL) was made from exponentially growing bacteria in fresh TSB media. 200 μL of this bacterial culture was added to each well of the microtiter plates. The plates were then incubated at 37°C for 24 h to allow biofilm formation. After that, media was removed gently, and the wells were washed with sterile 1× PBS to remove any unattached bacteria. Solution containing 20 μL of 10× peptide solution and 180 μL of fresh TSB were added. The plates were again incubated at 37°C for another 24 h. The extent of peptide disruption of biofilms was quantified using the same XTT method described above.

5.5. Hemolytic assays using human red blood cells

Hemolytic analysis of selected peptides was performed using an established protocol [14, 28]. Briefly, blood cells (UNMC Blood Bank) were washed three times with phosphate buffer saline (PBS) and diluted to a solution containing 0.5% or 2% blood cells. After peptide

treatment, incubation at 37°C for one hour, and centrifugation at 13,000 rpm, aliquots of the supernatant were transferred to a fresh 96-well microplate. To assess peptide cytotoxicity, the amount of hemoglobin released was measured at 545 nm. The percent lysis was calculated by assuming 100% release when human blood cells were treated with 1% Triton X-100, and 0% release when incubated with PBS buffer.

5.6. Cytotoxicity assays using human keratinocytes

Human keratinocytes from histologically normal skin (HaCaT cells; Fisher Cat # T0020001) were maintained in DMEM High Glucose media with 4 mM L-Glutamine (NyClone) and 100 U/mL penicillin, 100 μg/mL streptomycin (pen/strep) (Life Technologies), and 10% (v/v) inactivated fetal bovine serum (FBS) (NyClone). Cells were grown in 5% CO_2 at 37°C and were detached from culturing dish at 80% confluency using 0.025% trypsin-EDTA (NyClone) treatment. Peptide influence on the cell viability was estimated by using the MTS assay according to manufacturer's protocol (MTS, CellTiter96 AQ One Solution Cell Proliferation Assay, Promega).

5.7. LPS binding assays

The LPS (endotoxin) binding assay was carried out by utilizing the Pierce LAL Chromogenic Endotoxin Quantitation Kit (Thermo Scientific Cat No. 88282) [33]. Twenty-five microliter of serially diluted peptide solution and 25 μL of 4 U/mL of LPS were mixed in each well, and plates were incubated for 5 min at 37°C to allow the peptide to bind LPS. The mixture was then incubated for 10 min in the presence of 50 μL of amebocyte lysate reagent. Subsequently, 100 μL of the chromogenic substrate was added. Incubation was continued at 37°C for another 6 min and stopped with 50 μL of 25% acetic acid. The release of the product was monitored at 405 nm using a ChroMate 4300 Microplate Reader (GMI, Ramsey, MN). The percentage of LPS binding to the peptide at different concentrations was calculated from the control well without peptide.

5.8. Membrane permeation measurements

Fluorescence spectroscopy was used to follow bacterial killing. In brief, 10 μL of serially diluted 10× peptide ladders were made in 96-well corning COSTAR microtiter plates. Propidium iodide at a fixed concentration (20 μM) was added to each well followed by 88 μL of *S. aureus* USA300 or *E. coli* ATCC 25922 (with a final OD_{600} ~0.1) in TSB. The plate was finally incubated at 37°C with continuous shaking at 100 rpm in a FLUOstar Omega (BMG LABTECH Inc., NC, USA) microplate reader. The plate was read every 5 minutes for a total duration of 2 h with excitation and emission wavelengths of 584 nm and 620 nm, respectively.

In addition, the *E. coli* ML-35p strain was also utilized to probe the permeation of both the outer (OM) and inner membranes (IM) [30]. This strain was engineered to have two membrane reporters. Nitrocefin is used for detection of OM permeabilization. Nitrocefin is excluded from the periplasm. However, it enters the periplasmic space and gets cleaved by β-lactamase when bacterial OM is permeabilized by innate immune peptides. The chromogenic cleavage product was spectrophotometrically monitored at 490 nm. For IM permeation, *o*-nitrophenylgalactose (ONPG) is used as a reporter. ONPG is debarred to enter

cytoplasm due to the lack of the lac permease in this strain. However, permeabilization of the IM helps ONPG to enter cytoplasm and get cleaved by cytoplasmic β-galactosidase into *o*-nitrophenol, which can be detected spectrophotometrically at 420 nm. Experimentally, bacteria from an overnight culture, after re-inoculated into fresh TSB, were grown to the exponential phase at 37°C for 2 h with rotation at 220 rpm. After washing with 1× phosphate buffer saline (PBS) (GIBCO, Life Technologies Corporation, NY, USA), the culture was diluted to ~10^8 CFU/mL in PBS with 1% TSB. 70 μL of this culture was added to a 96-well microtiter plate (Corning COSTAR) containing increasing concentrations of peptide, 30 μM nitrocefin and 2.5 mM ONPG. Absorbances at both 490 nm and at 420 nm were monitored using FLUOstar Omega (BMG, Labtech, NC, USA) simultaneously. After shaking at 100 rpm, readings were taken every 2 min for a total of 40 min at 37°C. Data were plotted using the MARS data analysis software provided by the manufacturer.

5.9. In vivo efficacy studies

The potency of merecidin and 17BIPHE2 were tested *in vivo* using an established wax moth *Galleria mellonella* model.[31] The animals (~250 mg) were distributed by Timerline Live Pet Foods Marion, IL. Peptide in phosphate buffer (64 mg/kg) was injected 2 h prior to the infection with *S. aureus* USA300 at 10^6 CFU/moth. The animal groups included (1) untouched (no treatment), (2) PBS treated, (3) *S. aureus* USA300 infected at 10^6 CFU/moth without treatment, (4) *S. aureus* infected and treated with 17BIPHE2, and (5) *S. aureus* infected and treated with merecidin. Animals (10 per group) were kept at room temperature and observed daily to record live and dead ones.

5.10. Statistics

All experiments were replicated at least twice. For hemolysis, biofilm, cell viability and bactericidal colony counting experiments, plots represent the average values with standard deviation error bars. Membrane permeation experiments were duplicated for each condition and processed using the vendor's software (MARS, BMG Lab tech). For all the experiments, the level of significance was determined by performing paired Student t-test with parameters of two tailed distribution. p values > 0.05 were considered significant (*).

Supplementary Material

Refer to Web version on PubMed Central for supplementary material.

Acknowledgments

This work was supported by the National Institute of Allergy and Infectious Diseases of the National Institutes of Health (NIH) under Award Number R01AI105147 (PI: GW). The content is solely the responsibility of the authors and does not necessarily represent the official views of the NIH. During this study, XW was a visiting professor who was also supported by the China Scholarship Council.

References

1. Zasloff M. Antimicrobial peptides of multicellular organisms. Nature. 2002; 415:389–395. [PubMed: 11807545]
2. Hancock RE, Lehrer R. Cationic peptides: a new source of antibiotics. Trends Biotechnol. 1998; 16:82–88. [PubMed: 9487736]

3. Wang, G, editorAntimicrobial peptides: Discovery, Design and Novel Therapeutic Strategies (2nd version). CABI; Wallingford, England: 2017.
4. Wang G, Mishra B, Lau K, Lushnikova T, Golla R, Wang X. Antimicrobial peptides in 2014. Pharmaceuticals. 2015; 8:123–150. [PubMed: 25806720]
5. Epand RM, Vogel HJ. Diversity of antimicrobial peptides and their mechanisms of action. Biochim Biophys Acta. 1999; 1462:11–28. [PubMed: 10590300]
6. Morizane S, Gallo RL. Antimicorbial peptides in the pathogenesis of psoriasis. J Dermatol. 2012; 39:225–230. [PubMed: 22352846]
7. Wang G. Improved methods for classification, prediction, and design of antimicrobial peptides. Methods Mol Biol. 2015; 1268:43–66. [PubMed: 25555720]
8. Wang G, Li X, Wang Z. APD3: the antimicrobial peptide database as a tool for research and education. Nucleic Acids Res. 2016; 44:D1087–D1093. [PubMed: 26602694]
9. Fjell CD, Jenssen H, Hilpert K, Cheung WA, Panté N, Hancock RE, Cherkasov A. Identification of novel antibacterial peptides by chemoinformatics and machine learning. J Med Chem. 2009; 52:2006–2015. [PubMed: 19296598]
10. Li X, Li Y, Han H, Miller DW, Wang G. Solution structures of human LL-37 fragments and NMR-based identification of a minimal membrane-targeting antimicrobial and anticancer region. J Am Chem Soc. 2006; 128:5776–5785. [PubMed: 16637646]
11. Mishra B, Wang G. *Ab initio* design of potent anti-MRSA peptides based on database filtering technology. J Am Chem Soc. 2012; 134:12426–12429. [PubMed: 22803960]
12. Rathinakumar R, Walkenhorst WF, Wimley WC. Broad-spectrum antimicrobial peptides by rational combinatorial design and high-throughput screening: the importance of interfacial activity. J Am Chem Soc. 2009; 131:7609–7617. [PubMed: 19445503]
13. de Breij A, Riool M, Cordfunke RA, Malanovic N, de Boer L, Koning RI, Ravensbergen E, Franken M, van der Heijde T, Boekema BK, Kwakman PHS, Kamp N, El Ghalbzouri A, Lohner K, Zaat SAJ, Drijfhout JW, Nibbering PH. The antimicrobial peptide SAAP-148 combats drug-resistant bacteria and biofilms. Sci Transl Med. 2018; 10:eaan4044. [PubMed: 29321257]
14. Wang G, Hanke ML, Mishra B, Lushnikova T, Heim CE, Chittezham Thomas V, Bayles KW, Kielian T. Transformation of Human Cathelicidin LL-37 into Selective, Stable, and Potent Antimicrobial Compounds. ACS Chem Biol. 2014; 9:1997–2002. [PubMed: 25061850]
15. Hsieh I, Hartshorn KL. The Role of Antimicrobial Peptides in Influenza Virus Infection and Their Potential as Antiviral and Immunomodulatory Therapy. Pharmaceuticals. 2016; 9:53.
16. Wang G, Mishra B, Epand RF, Epand RM. High-quality 3D structures shine light on antibacterial, anti-biofilm and antiviral activities of human cathelicidin LL-37 and its fragments. Biochim Biophys Acta. 2014; 1838:2160–2172. [PubMed: 24463069]
17. Oren Z, Lerman JC, Gudmundsson GH, Agerberth B, Shai Y. Structure and organization of the human antimicrobial peptide LL-37 in phospholipid membranes: relevance to the molecular basis for its non-cell-selective activity. Biochem J. 1999; 341(Pt 3):501–513. [PubMed: 10417311]
18. Kuroda K, Okumura K, Isogai H, Isogai E. The Human Cathelicidin Antimicrobial Peptide LL-37 and Mimics are Potential Anticancer Drugs. Front Oncol. 2015; 5:144. [PubMed: 26175965]
19. Nijnik A, Hancock RE. The roles of cathelicidin LL-37 in immune defences and novel clinical applications. Curr Opin Hematol. 2009; 16:41–47. [PubMed: 19068548]
20. Duplantier AJ, van Hoek ML. The Human Cathelicidin Antimicrobial Peptide LL-37 as a Potential Treatment for Polymicrobial Infected Wounds. Front Immunol. 2013; 4:143. [PubMed: 23840194]
21. Wang G, Waston K, Buckheit R Jr. Anti-human immunodeficiency virus type 1 activities of antimicrobial peptides derived from human and bovine cathelicidins. Antimicrob Agents Chemother. 2008; 52:3438–3440. [PubMed: 18591279]
22. Wang G, Epand RF, Mishra B, Lushnikova T, Thomas VC, Bayles KW, Epand RM. Decoding the functional roles of cationic side chains of the major antimicrobial region of human cathelicidin LL-37. Antimicrob Agents Chemother. 2012; 56:845–856. [PubMed: 22083479]
23. Epand RF, Wang G, Berno B, Epand RM. Lipid segregation explains selective toxicity of a series of fragments derived from the human cathelicidin LL-37. Antimicrob Agents Chemother. 2009; 53:3705–3714. [PubMed: 19581460]

24. Mishra B, Golla MR, Lau K, Lushnikova T, Wang G. Anti-Staphylococcal Biofilm Effects of Human Cathelicidin Peptides. ACS Med Chem Lett. 2016; 7:117–121. [PubMed: 26819677]
25. Mishra B, Wang G. Individual and combined effects of engineered peptides and antibiotics on the *Pseudomonas aeruginosa* biofilms. Pharmaceuticals. 2017; 10:58.
26. Abou Alaiwa MH, Reznikov LR, Gansemer ND, Sheets KA, Horswill AR, Stoltz DA, Zabner J, Welsh MJ. pH modulates the activity and synergism of the airway surface liquid antimicrobials β-defensin-3 and LL-37. Proc Natl Acad Sci USA. 2014; 111:18703–8. [PubMed: 25512526]
27. Morgera F, Vaccari L, Antcheva N, Scaini D, Pacor S, Tossi A. Primate cathelicidin orthologues display different structures and membrane interactions. Biochem J. 2009; 417:727–35. [PubMed: 18922132]
28. Dean SN, Bishop BM, van Hoek ML. Natural and synthetic cathelicidin peptides with anti-microbial and antibiofilm activity against *Staphylococcus aureus*. BMC Microbiol. 2011; 11:114. [PubMed: 21605457]
29. Overhage J, Campisano A, Bains M, Torfs EC, Rehm BH, Hancock RE. Human host defense peptide LL-37 prevents bacterial biofilm formation. Infect Immun. 2008; 76:4176–82. [PubMed: 18591225]
30. Lehrer RI, Barton A, Ganz T. Concurrent assessment of inner and outer membrane permeabilization and bacteriolysis activity in *E. coli* by multiple-wavelength spectroscopy. J Immunol Methods. 1988; 108:153–158. [PubMed: 3127470]
31. Ramarao N, Nielsen-Leroux C, Lereclus D. The insect *Galleria mellonella* as a powerful infection model to investigate bacterial pathogenesis. J Vis Exp. 2012; (70):e4392. [PubMed: 23271509]
32. Wang G. Structures of human host defense cathelicidin LL-37 and its smallest antimicrobial peptide KR-12 in lipid micelles. J Biol Chem. 2008; 283:32637–32643. [PubMed: 18818205]
33. Turner J, Cho Y, Dinh N-N, Waring AJ, Lehrer RI. Activities of LL-37, a cathelin-associated antimicrobial peptide of human neutrophils. Antimicrob Agents Chemother. 1998; 42:2206–2214. [PubMed: 9736536]
34. Mishra B, Epand RF, Epand RM, Wang G. Structural location determines functional roles of the basic amino acids of KR-12, the smallest antimicrobial peptide from human cathelicidin LL-37. RSC Adv. 2013; 3:19560–71.
35. Wang X, Bozelli JC Jr, Mishra B, Lushnikova T, Epand RM, Wang G. Arginine-lysine Positional Swap of the LL-37 Peptides Reveals Evolutional Advantages of the Native Sequence and Leads to Bacterial Probes. Biochim Biophys Acta. 2017; 1859:1350–1361.
36. Wang G. Determination of solution structure and lipid micelle location of an engineered membrane peptide by using one NMR experiment and one sample. Biochim Biophys Acta. 2007; 1768:3271–3281. [PubMed: 17905196]
37. Clinical and Laboratory Standards Institute. M27-A3. Reference method for broth dilution antifungal susceptibility testing of yeasts. 3. 2008. Approved standard

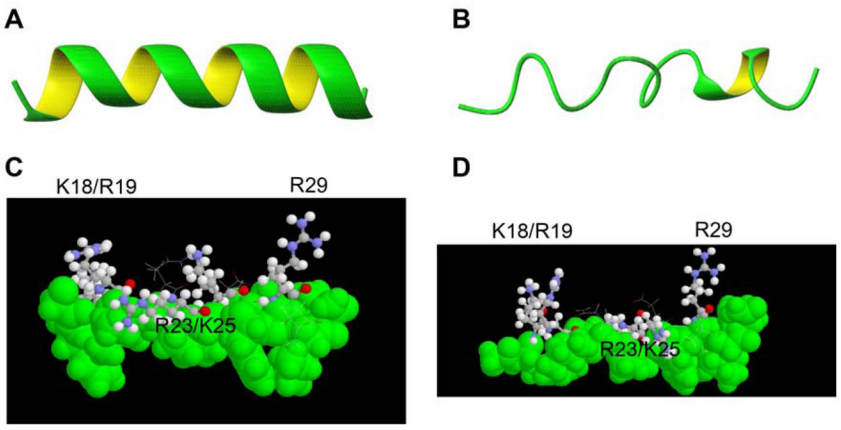

Figure 1.

Three-dimensional (3D) amphipathic structures (A–D) of a helical peptide GF-17 (left panels) and a non-helical peptide 17BIPHE2 (right panels), derived from the major antimicrobial region (residues 17–32) of human LL-37. Ribbon diagrams are depicted in panels A and B. In the space-filling models (C & D), hydrophobic residues (space-filling model) are in green, while hydrophilic basic side chains are displayed in the ball-and-stick model. Amino acids in the two peptides are numbered as in human LL-37 (sequence LLGDFFRKSKEKIGKEFKRIVQRIKDFLRNLVPRTES), where residues 17–32 are underlined. PDB ID for GF-17 is 2L5M[22].

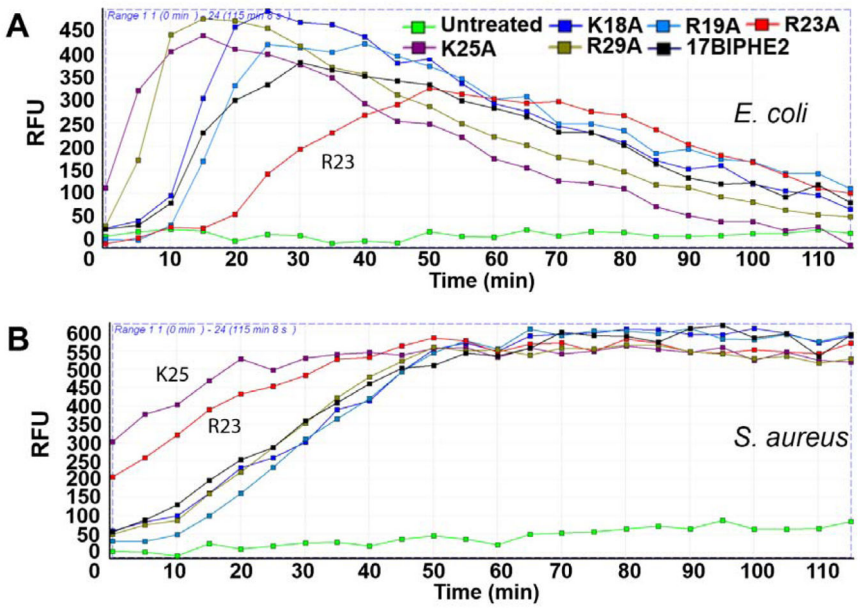

Figure 2.

Membrane permeation of *E. coli* ATCC 259922 (A) and *S. aureus* USA300 (B) by 17BIPHE2 and its alanine variants (6.25 μM) in the presence of propidium iodide. Note that the R23A variant (red) is the poorest in the case of *E. coli* but better than the wild type (black) in the case of *S. aureus*. Relative fluorescence units (y axis) are abbreviated as RFU in the figure.

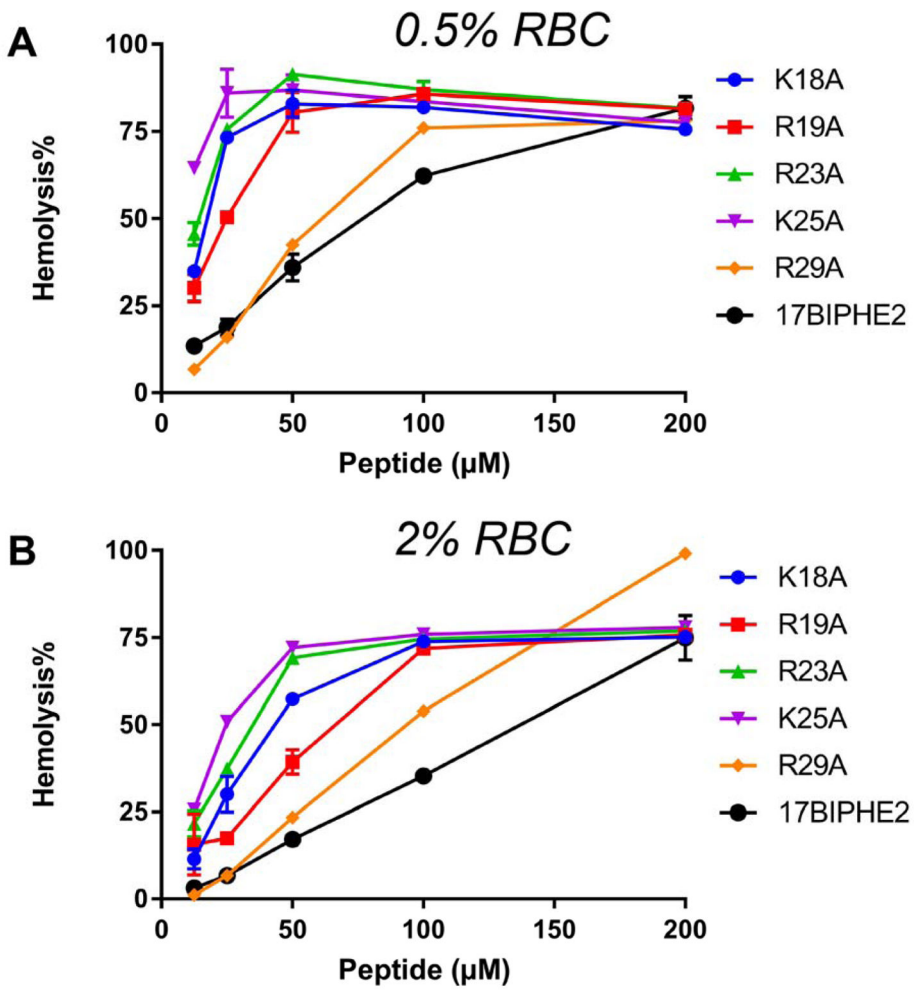

Figure 3.

Hemolysis of 0.5% (A) and 2% (B) human red blood cells by 17BIPHE2 and its single alanine variants at various concentrations.

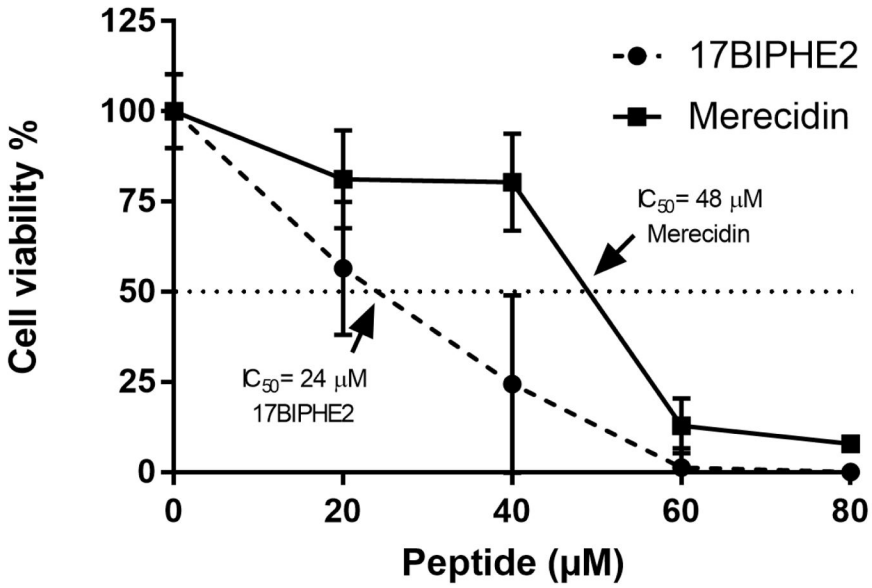

Figure 4.

Cell viability of human HaCaT cells after treating with various concentrations of 17BIPHE2 (dotted line) and merecidin (solid line). Experiments were conducted in duplicates and average results were reported. The error bars represent the standard deviation of the values from the mean. The level of significance was determined by performing Student t-Test with parameters of one tailed distribution with samples of equal variance (*: $p < 0.05$; **: $p < 0.005$ and ***: $p < 0.0005$).

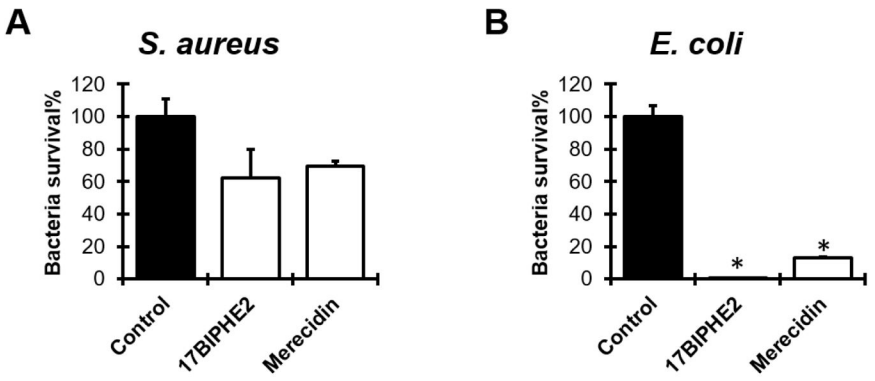

Figure 5.

Survival rates of *S. aureus* USA300 (A) and *E. coli* ATCC 25922 (B) determined by colony counting after killing with 17BIPHE2 or merecidin for 15 min followed by plating on Luria-Bertani agar plates. The colonies were counted after overnight incubation at 37°C. Data from the duplicated experiments were processed as described in Figure 4.

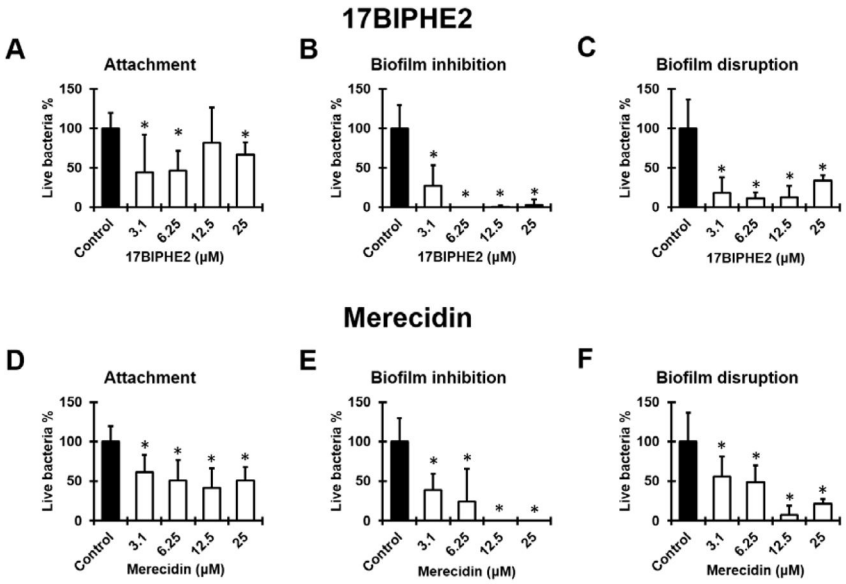

Figure 6.

Antibiofilm capability of 17BIPHE2 (A–C) and merecidin (D–F) against *S. aureus* USA300 bacterial adhesion (A & D), biofilm growth (B & E), and the 24 h biofilms (C & F). Data from the duplicated experiments were processed as described in Figure 4.

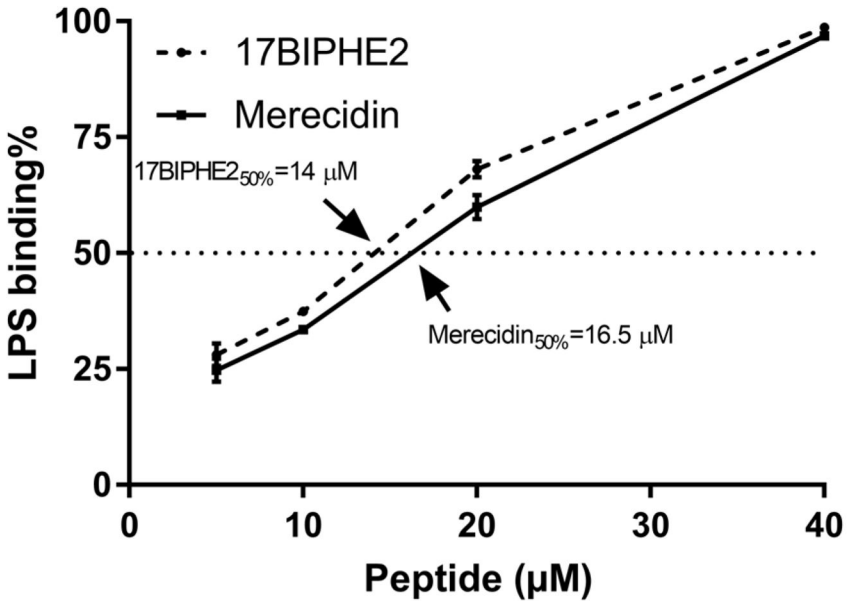

Figure 7.

LPS binding of 17BIPHE2 (dotted line) and merecidin (solid line). Peptide concentrations for 50% LPS binding are indicated. For further details, see the Method. Data from the duplicated experiments were processed as described in Figure 4.

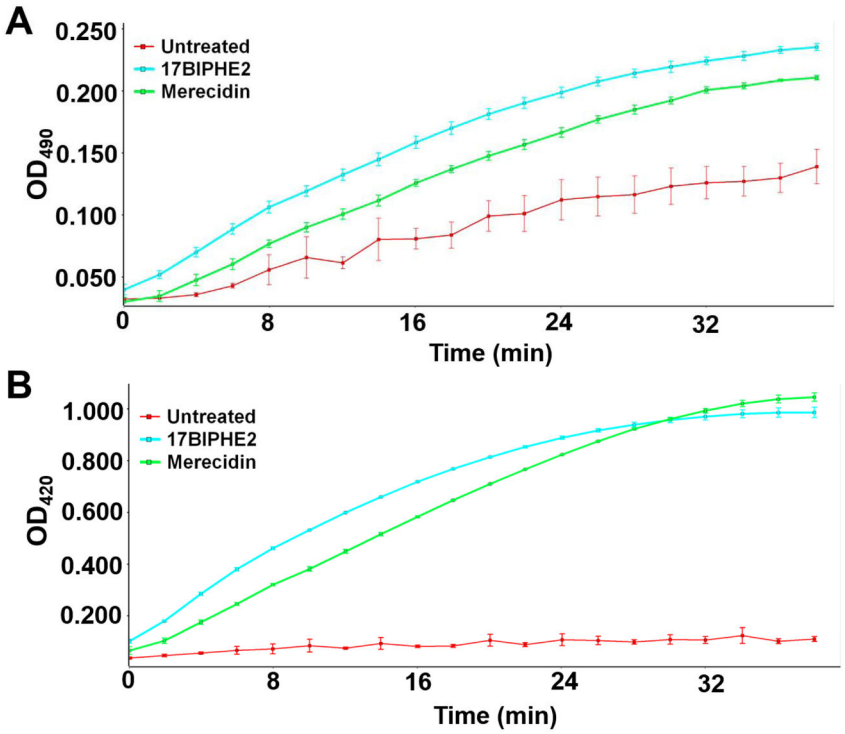

Figure 8.

Simultaneous probing permeation of (**A**) the outer (OM) and (**B**) inner membranes (IM) of *E. coli* ML35p by 17BIPHE2 (blue) and merecidin (green). The peptides were treated at 6.25 μM and the absorbance was recorded for 40 mins. There is an increase in absorbance in both cases relative to the untreated bacteria (red). Experiments were duplicated and processed using the vendor's software.

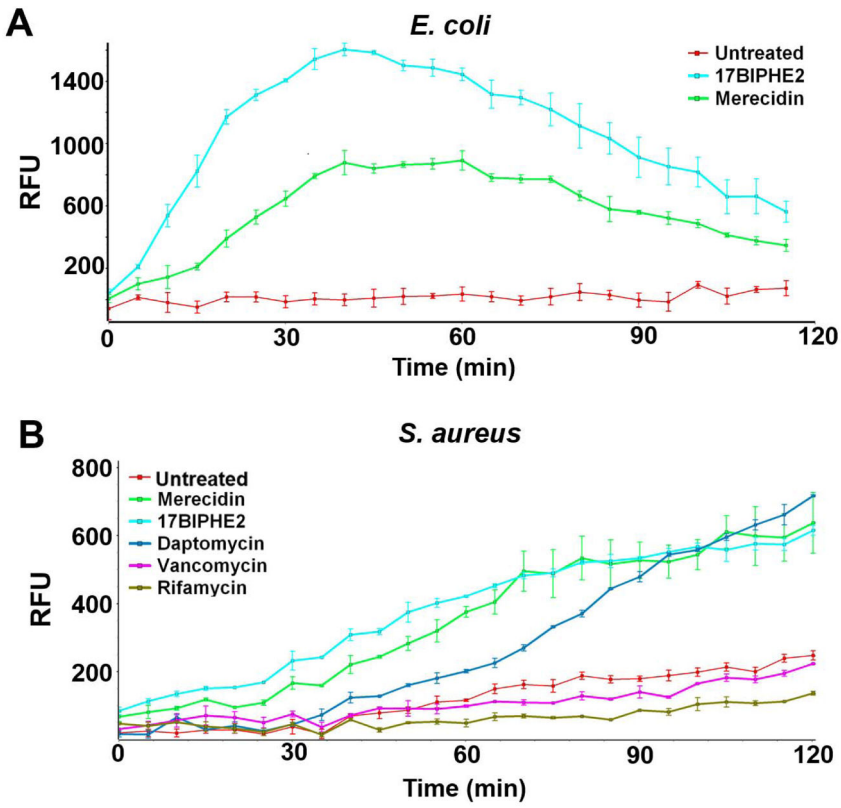

Figure 9.

Membrane permeation of *E. coli* ATCC 25922 (A) and *S. aureus* USA300 (B) by 17BIPHE2 (black) and merecidin (green) as indicated by the propidium iodide (PI) probe. In panel A, the bacteria were treated at a peptide concentration of 6.2 μM. In panel (B), the peptide concentrations are 3.1 μM and the antibiotics were treated at their MIC values: daptomycin (gold) at 0.78 μM; vancomycin (purple) at 0.78 μM; and rifamycin (light green) at 0.2 μM. The concentration of the PI dye, as well as excitation and emission wavelengths, is given in Materials and Methods. Experiments were duplicated and processed using the vendor's software. Relative fluorescence units (y axis) are abbreviated as RFU in the figure.

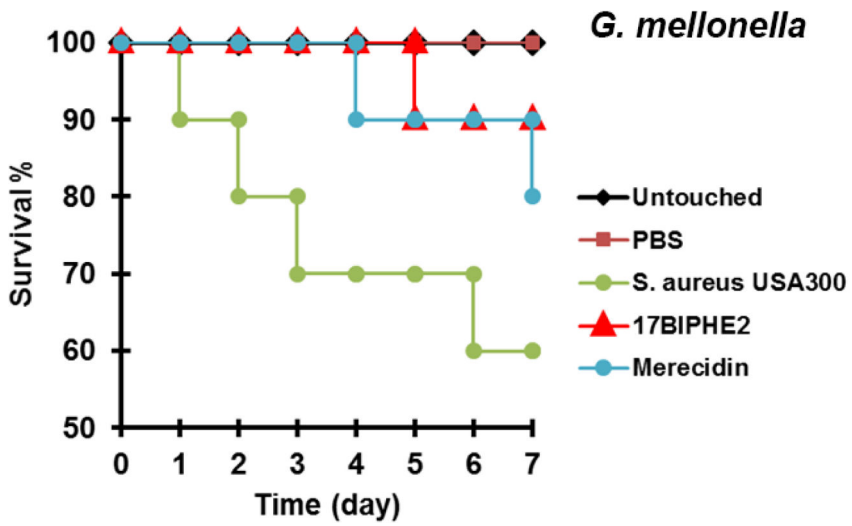

Figure 10.

Protection of wax moths (*Galleria mellonella*) from *S. aureus* USA300 infection by designer peptides 17BIPHE2 and merecidin based on human cathelicidin LL-37.

Table 1

Minimal inhibitory and hemolytic concentrations (MIC and HL_{50} in μM) of 17BIPHE2 and its alanine variants (group 1 peptides) against various bacteria [a]

	EC [b]	PA	USA300	UAMS-1	AB	KP	EF	SE	HL_{50} [c]
17BIPHE2	3.1	6.25	3.1	≤ 3.1	3.1	3.1	25	1.6	90
17BIPHE2-K18A	3.1	12.5	3.1	6.25	6.25	3.1	6.25–12.5	1.6	18
17BIPHE2-R19A	6.25	12.5	3.1	6.25	6.25	3.1	12.5	1.6	25
17BIPHE2-R23A	6.25–12.5	6.25	3.1	6.25	6.25	3.1	12.5	1.6	14
17BIPHE2-K25A	6.25	12.5	3.1–6.25	6.25	6.25	3.1	12.5	1.6	<12.5
17BIPHE2-R29A	3.1	6.25	3.1–6.25	6.25	6.25	3.1	12.5	3.1	62
17BIPHE2-2KA [d]	6.25–12.5	25	3.1	12.5	25	3.1–6.25	12.5	1.6	<12.5
17BIPHE2-3RA	> 50	> 50	6.25	> 50	>50	>50	>25	6.25	<12.5

[a] Peptide amino acid sequences and properties are listed in supporting Table S1;

[b] EC: *E. coli* ATCC 25922; PA, *P. aeruginosa* PAO1; USA300, *S. aureus* USA300; UAMS-1, *S. aureus* UAMS-1; AB, *A. baumannii* B28-16; KP, *K. pneumoniae* ATCC 13883; EF, *Enterococcus faecium* ATCC 51559; SE, *S. epidermidis* 1457.

[c] HL_{50} was calculated based on the 0.5% RBC, which appeared to be slightly more hemolytic than those observed at 2%.

[d] 2KA means the replacement of K18 and K25 of 17BIPHE2 with alanines and the three arginines in 3RA were changed to alanines.

Table 2

Bacterial minimal inhibitory concentration, hemolytic ability, and cell selectivity index of group 2 peptides

Peptide [a]	MIC (μM) [b]				HL_{50} [c] (μM)	CSI [c]
	EC	*PA*	*KP*	*SA*		
17BIPHE2	3.1	6.2	3.1	3.1	110	35
17BIPHE2-V21A	3.1–6.2	6.2	12.5	3.1	80	26
17BIPHE2-R23A	6.2–12.5	6.2	3.1	3.1	25	8
17BIPHE2-R23S	6.2	12.5	12.5	6.2	110	18
17BIPHE2-R23O (merecidin)	3.1	6.2	12.5	3.1	300	97

[a]The C-termini of these peptides are amidated. Peptide sequence and properties are provided in Figure S1.

[b]The minimal inhibitory concentration (MIC) against SA, *S. aureus* USA300; EC, *E. coli* ATCC 25922; PA, *P. aeruginosa* PAO1; and KP, *Klebsiella pneumoniae*.

[c]Cell selectivity index (CSI) of the peptide was calculated using the 50% hemolytic concentration HL_{50} divided by the MIC of *S. aureus* USA300. The higher the CSI value, the better the cell selectivity of the peptide. The HL_{50} for 17BIPHE2 in this table differs from that reported previously [14], probably due to different batches of red blood cells or the use of different concentration of cells (see Figure 3).

Table 3

Statistics of natural antimicrobial peptides against Gram-positive or Gram-negative bacteria collected in the Antimicrobial Peptide Database[1]

Antimicrobial Activity	Gram-negative bacteria	Gram-positive bacteria
Total number of peptides	269	485
Average net charge	+3.29	+2.40
Average hydrophobic%	36.26	42.69
Lysine%	9.26	7.47

[1]Accessed in November 2017 at http://aps.unmc.edu/AP) [8].